

APPLIED RESEARCH

Application of Optimized Grey-Markov Model to Land Subsidence Monitoring With InSAR

DEBAO YUAN, LIBIAO ZHANG, RUOPENG YAN, LING WU, YANYAN FENG, AND LUYI FENG

Department of Geomatics Engineering, China University of Mining and Technology (Beijing), Beijing 100083, China

Corresponding author: Debao Yuan (yuandb@cumtb.edu.cn)

This work was supported in part by the National Natural Science Foundation of China under Grant 52174160 and in part by the Natural Science Foundation of Hebei Province under Grant EE2020402086.

ABSTRACT Land subsidence prediction in mining areas is one of the most important applications of land deformation monitoring, which is significance for safe production. We used interferometric point target analysis (IPTA) timing series interferometry synthetic aperture radar (InSAR) processing technology to analyze the land subsidence results for the Xinfu mining area from 2017 to 2020; and compared them to global positioning system (GPS) static monitoring data. We proposed a residual correction theory based on deviation coefficient using the grey prediction and Markov models, and an optimized Grey-Markov model (RGM-M model) was established to predict the land subsidence of the mining area. Our results show that: (1) The maximum difference between InSAR timing processing results and GPS monitoring data in the same period is 10.91mm; they have roughly the same subsidence trend, indicating that IPTA timing series InSAR technology are strongly reliable in mining deformation. (2) Compared to the traditional Grey-Markov model, the improved residual correction and dynamic assignment of the Grey-Markov model improves the prediction accuracy. The optimized residual correction and dynamic empowerment of the Grey-Markov model prediction results are more suitable for the actual fluctuation of land subsidence value in the mining area. The maximum root mean square error of the prediction results is 0.751mm, and the maximum average absolute percentage error is 7.46%, which has a certain guiding significance for the work of monitoring, prediction and safety management of land deformation in the mining area.


INDEX TERMS Dynamic empowerment, Grey-Markov model, mining subsidence, prediction, residual correction, timing series InSAR.

I. INTRODUCTION

Since modern times, coal has been one of the main energy sources of human society. Therefore, the safety production of mining areas has widely concerned all walks of life. Research on monitoring and predicting land subsidence in mining areas has always been a prominent issue [1]. In the field of land subsidence monitoring in mining areas, there are many traditional monitoring methods and means, such as theodolite triangle elevation measurement; and high-grade precision leveling to full station measurement; and global positioning navigation system (GPS) positioning measurement, etc. The need to establish monitoring stations along with the mining deformation; through repeated field observation; is

time-consuming; with input cost, especially since the labor cost is also higher; furthermore, it is too complex for some terrain, has inaccessible areas, and it is too difficult to establish observation stations and measurement work.

In the past few decades, InSAR has become unanimously recognized as important monitoring means in this field [2]. InSAR technology is one of the most popular research fields. With the development of commercial satellites in recent years, more and more commercial SAR satellite data have been applied to land subsidence monitoring, achieving the expected results. The main advantage of using InSAR technology for imaging is continuous no interval observation, high accuracy and resolution, wide coverage, and low cost. It has been used in various fields of national economic development; for example, InSAR technology is used for building ground DEM models, land subsidence monitoring, volcano,

The associate editor coordinating the review of this manuscript and approving it for publication was John Xun Yang .

earthquake, landslide, and other natural disasters [3], [4], [5], [6].

In recent years, there have been increasingly scientific studies and case applications of land subsidence monitoring in mining areas, and the technology is becoming more mature [7]. In addition to InSAR technology, many new technologies such as continuous operation reference station system (CORS) satellite positioning service, laser 3D scanning technology, and mining ground subsidence monitoring systems based on geographic information system (GIS) technology are also used in mining deformation. By contrast, the use of InSAR technology to monitor the land deformation of the mining area obtains a range of high-precision monitoring data; and effectively reduces manpower and material resources, reducing the great cost and investment, and completing the continuous real-time monitoring of the whole mining area [6], [9]. With the continuous break-through and improved timing of InSAR technology in recent years, highly accurate deformation information can be obtained theoretically, and the accuracy of its data processing results can reach the centimeter-level [7], [10], [11]. Therefore, we can research and work on land subsidence prediction through InSAR technology.

The IPTA timing series InSAR data processing method is a coherent target point timing analysis method based on GAMMA software. Combining two persistent scatterer (PS) InSAR and small baseline subset (SBAS) InSAR technologies; and adopting the PS-InSAR process, helps to realize the independent selection of the SBAS-InSAR technology for the baseline set. Meanwhile, during the entire InSAR timing process, the InSAR time sequence processes the whole process; with free and controllable parameters, providing high degrees of freedom and processing space for InSAR data processing [8], [9]. Therefore, the processing personnel can really handle the process freely according to the situation and actual image data. The practical accuracy and application reliability of InSAR data processing improves on the restrictions of modular integrated processing in other processing software and methods [15].

Grey model is a new prediction method that can use less data to predict an uncertain system [16]. GM (1,1) model is the simplest and most important prediction model with only one variable and first-order differential. It is one of the most basic and important prediction models in the Grey theory system. [17]. However, in practice, emergent and uncontrollable factors can affect land subsidence data, and raw data sequences have inevitable volatility. Residual correction models optimized according to residual weight can theoretically be improved with the original data sequence based on different original data sequence conditions, thereby improving the prediction accuracy of the Grey model. The prediction process of the Markov model has strong randomness, which evolved from the Markov stochastic prediction chain, first proposed by the Russian mathematician Markov in 1907 [18], [19]. In known states, the future evolution of the Markov model is completely unrelated to what occurred

previously, namely that the evolutionary direction is not based on past changes. This paper uses dynamic empowerment; and data values after each Grey-Markov model prediction was added to the calculated sample of the next evaluation weight matrix. A dynamic Markov evaluation weight matrix is established, more scientific in theory. Four typical subsidence points in the subsidence data of the new and spring exploration areas were replaced with the traditional GM (1,1) model, Grey-Markov combination prediction model with optimized residual correction, and dynamic empowerment of the Grey-Markov combination model. We compared and analyzed the prediction results. The results showed the optimized Grey-Markov model predicts the trend and subsidence value of land subsidence more accurately than the traditional Grey-Markov combination model. These results have good application prospects for mine land subsidence monitoring, prediction, and safety management.

II. METHODS

A. STUDY AREA

The main research area of this paper is the new exploration area in the Wuzhong City, Ningxia Province, China. It is located at 70km southeast of Wuzhong City. The exploration area is about 4.17KM long from north to south and 2.22km wide from east to west. The specific scope is shown in Figure 1. The landform is mainly mountainous, with dry climate and four distinct seasons.

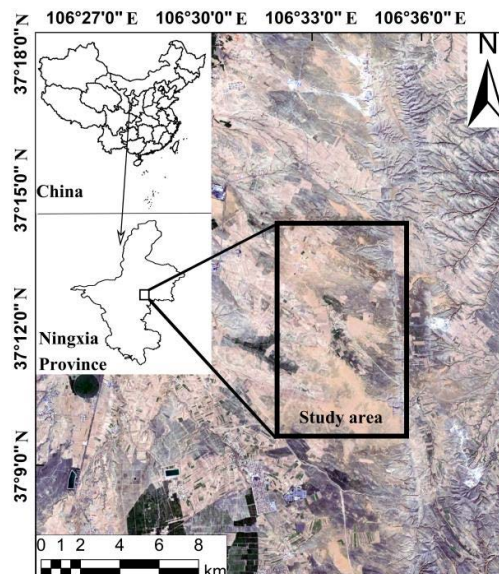


FIGURE 1. The map of study area.

B. DATA

The data used in this paper include SAR images captured by the Sentinel-1A satellite. The Sentinel-1 satellite is a C-band Earth observation satellite launched by ESA in the Copernican Program. It consists of two satellites, A and B satellite. Each satellite has a separate return period of 12 days and a binary return period of 6 days. It's main working mode is the interference wide amplitude (IW) scanning imaging

mode; the SAR image data width reaches 250km. The orbital data parameters are shown in Table 1.

TABLE 1. Track data parameters.

Revisit Cycle (day)	Imaging mode	Wave length	Wave band	Track number
12	IW	5.6cm	C band	162

In this study, we collected 114 SLC data from Sentinel-1 A satellite ascending orbit images covering the study area. The image time distribution was from 14 January 2017 to 24 December 2020. The DEM data used was SRTM data with an accuracy of 30m.

III. IPTA TIMING SERIES INSAR PROCESSING

Interferometric Persistent Target Analysis (IPTA) is a fusion of PS-InSAR technology and SBAS-InSAR technology during data processing. Since the traditional InSAR analysis technology is in view of the land; and prone to the loss correlation effect, the point target, as a reference for the timing analysis, does not involve analyzing interference stripes. Therefore, errors caused by incoherence are avoidable. The basic principle is to perform sequential InSAR processing of several acquired SAR images analyze the phase and amplitude specific information of the obtained points, identify some relatively stable target points, such as buildings, rocks, road lands, and even previously installed artificial angle reflectors. Since these point targets are relatively stable, the high echo signal intensity can maintain its relatively stable ground reflection properties for a considerable time [11]. IPTA timing analysis technology calculates the value change in elevation information and the positive value of the deformation rate. It removes the atmospheric phase; and obtains the sequential land deformation information based on these stable coherence points. In addition, during IPTA timing processing, combined with the baseline selection of SBAS-InSAR technology, the length of image data pairs can be freely selected. Similar to SBAS-InSAR processing technology, the small baseline set can also be selected; for subsequent processing. During processing (using the Gamma software, for example), the IPTA module; is integrated into the software. From the SAR image data registration to solving the land deformation information, hundreds of parameters are involved in IPTA timing processing technology. For example, the detailed parameters of multi-view processing, the length range of spatial and temporal baseline selection, the specific parameters of difference processing, the window size of filtering processing, the coherence coefficient of point selection, and other specific point selection criteria. These parameters are free and controllable. By entering the control mode of the script commands, traditional InSAR data processing (such as SARscape, etc.); relies solely on manually clicking the operation page. The dilemma of immobilizing many processing parameters; through the flexible regulation of various parameters; accomplishes more accurate data processing. The

solution parameters must be adjusted according to the actual situation. Thus, the solution accuracy improves. At the same time, IPTA timing processing technology also depends on certain requirements related to the experience level of the data processors.

During timing processing, the interference phase in the interference stripe diagram generated by any two images mainly includes five parts, namely, the topographic phase, land deformation phase, flat land phase, atmospheric delay phase and noise phase. During IPTA processing:

$$\varphi = \varphi_{top} + \varphi_f + \varphi_{def} + \varphi_{atm} + \varphi_n \quad (1)$$

In the formula, φ is the interference phase of the target point; φ_{top} is the interference phase due to topographic elevation; φ_f is the flat phase, which can be calculated from the geometric relationship of image imaging; φ_{def} is the line of sight to radar (LOS); φ_{atm} represents the noise phase caused by the atmospheric delay; and φ_n represents the system thermal noise phase.

φ_{top} and φ_f can be removed after the differential interference treatment, to obtain the differential phase φ_{diff} :

$$\varphi_{diff} = \varphi_{def} + \varphi_{tope} + \delta\varphi_{atm} + \delta\varphi_n \quad (2)$$

φ_{tope} is the elevation error phase. The required land deformation information can finally be extracted from the separated φ_{def} :

$$\varphi_{tope} = -\frac{4\pi B_{\perp}}{\lambda R \sin \theta} \Delta h \quad (3)$$

v represents the linear deformation rate of coherence points relative to the reference point; t represents the time baseline; and φ_{def_n} is the nonlinear deformation phase.

The IPTA method uses the two-dimensional linear phase solution model, that is, through continuous regression iterative calculation; to complete the separation and removal of various errors, obtaining the deformation rate. In this iteration process, the Delaunay triangle network and Minimum cost flow (MCF) algorithm can solve the phase disentanglement of the target.

IV. THE IMPROVED GREY-MARKOV MODEL

A. THEORY OF GREY MODEL

The Grey system prediction refers to predicting the eigenvalue changes of system behavior. It includes system predictions known and uncertain information. In other words, the Grey process changes within a certain threshold range related to the time series [20], [21]. The phenomena shown in the ash process are random and fluctuating; however, they are also orderly and bounded, so the data set has an underlying law. The Grey system prediction model uses this potential law to establish the Grey model, fulfilling the prediction of the Grey system [17], [22], [23].

The Grey model was established as follows:

(1) The original data sequence that corresponds to time is $x^{(0)}$:

$$x^{(0)} = \{x^{(0)}(1), x^{(0)}(2), \dots, x^{(0)}(n)\} \quad (4)$$

(2) To reduce the dynamic randomness of the data, the raw data sequence is accumulated:

$$x^{(1)} = \sum_{i=1}^k x^{(0)}(i), \quad k = 1, 2, \dots, n \quad (5)$$

$$x^{(1)} = \{x^{(1)}(1), x^{(1)}(2), \dots, x^{(1)}(n)\} \quad (6)$$

(3) Build the adjacent mean sequence:

$$y^{(1)}(k) = \frac{1}{2} \{x^{(1)}(k) + x^{(1)}(k-1)\}, \quad k \geq 2 \quad (7)$$

Adjacent to the mean is the whitening background value $y^{(1)}(k)$.

(4) Construction of the white-chemical differential equation:

$$\frac{dx^{(1)}}{dt} + ax^{(1)} = u \quad (8)$$

By least squares, the following calculation is available:

$$\hat{a} = (B^T B)^{-1} B^T Y \quad (9)$$

$$B = \begin{bmatrix} -y^{(1)}(2) & 1 \\ -y^{(1)}(3) & 1 \\ \vdots & \vdots \\ -y^{(1)}(n) & 1 \end{bmatrix}, \quad Y = \begin{bmatrix} x^{(0)}(2) \\ x^{(0)}(3) \\ \vdots \\ x^{(0)}(n) \end{bmatrix} \quad (10)$$

(5) Solve the response equation:

$$\hat{x}^{(1)}(k+1) = \left(x^{(0)}(1) - \frac{u}{a}\right) e^{-ak}, \quad k = 1, 2, \dots, n-1 \quad (11)$$

(6) From the reduction of reduction:

$$x^{(0)}(k) = x^{(1)}(k) - x^{(1)}(k-1) \quad (12)$$

when $k = 1$,

$$\hat{x}^{(0)}(0) = \hat{x}^{(1)}(1) = \hat{x}^{(0)}(1) \quad (13)$$

when $2 \leq k \leq n$,

$$x^{(0)}(k) = (1 - e^a) \left(x^{(0)}(1) - \frac{u}{a}\right) e^{-u(k-1)} \quad (14)$$

(7) Model accuracy test:

For GM (1,1) model, the mean variance ratio (C) and small probability error (Δ), are used to determine the quality of the model [24]. The inspection criteria are shown in Table 2.

Test of mean variance ratio: the variance of the original data, and variance of the residual columns are:

$$S_1^2 = \frac{1}{n-1} \sum_{k=1}^n \left(x^{(0)}(k) - \bar{x}^{(0)}\right)^2 \quad (15)$$

$$S_2^2 = \frac{1}{n-1} \sum_{k=2}^n \left(\varepsilon^{(0)}(k) - \bar{\varepsilon}^{(0)}\right)^2 \quad (16)$$

where, $x^{(0)}(k)$ is the original data sequence; $\bar{x}^{(0)}$ represents the original data sequence mean; $\varepsilon^{(0)}(k)$ is the residual sequence; and $\bar{\varepsilon}^{(0)}$ is the residual sequence mean.

The Model is considered qualified if it meets these two requirements.

TABLE 2. Test standard of model accuracy.

Prediction accuracy	Mean variance ratio (C)	Small probability error (Δ)
Excellent (Level I)	$C \leq 0.35$	$\Delta \geq 0.95$
Qualified (Level II)	$0.35 < C \leq 0.5$	$0.8 \leq \Delta < 0.95$
Barely qualified (Level III)	$0.5 < C \leq 0.65$	$0.7 \leq \Delta < 0.85$
Non-qualified (Level IV)	$C > 0.65$	$\Delta < 0.7$

B. THEORY OF MARKOV MODEL

The Markov model was proposed by the Russian mathematician Markov. It includes a dynamic change process with randomness; called the Markov chain. The Markov transfer process only relates directly to the previously connected data; and not to other past data, known as ‘‘post-invalid’’ [25]. The expression is:

$$x_{(k+1)} = x_{(k)} \cdot P \quad (17)$$

The Markov model divides the data into several different state intervals (for both prediction accuracy and data complexity, generally divided into 3-4 data), and finds the optimal state step by step using the state transfer matrix; to estimate future changes.

1) STATUS DIVISION

Using the ratio of the fitted predicted value of the GM (1,1) model to the actual land subsidence monitoring data as a reference, the fitted data of the GM (1,1) model is divided into three state intervals according to this ratio, expressed by $S_i \in [a_i, b_i], i = 1, 2, \dots, n$. The lower and upper limits of the interval are a_i, b_i . The transfer probability from state S_i to state S_j by k steps is expressed as:

$$P_{ij}^k = \frac{n_{ij}^k}{n_i} \quad (18)$$

where k represents the steps from S_i to S_j ; P_{ij}^k indicates the probability from state S_i to S_j after k steps; n_i represents the number of samples in S_i ; and n_{ij}^k represents the number of samples from state S_i to S_j after k steps.

2) CONSTRUCT THE STATE TRANSITION MATRIX

The state transition matrix consisting of state transition probability is:

$$P^{(k)} = \begin{bmatrix} P_{11}^k & P_{12}^k & \dots & P_{1n}^k \\ P_{21}^k & P_{22}^k & \dots & P_{2n}^k \\ \vdots & \vdots & \ddots & \vdots \\ P_{n1}^k & P_{n2}^k & \dots & P_{nn}^k \end{bmatrix} \quad (19)$$

3) DETERMINE THE OPTIMAL VALUE

The matrix $P(k)$ is the state corresponding to the maximum value of the column vector sum in the state list of row vectors [26]. In other words, Markov’s ideal state. The optimized

forecast value is:

$$y^{(0)}(i+1) = \frac{1}{2}(a_i + b_i)\hat{x}^{(0)}(i+1) \quad (20)$$

where the final optimized prediction value is $y^{(0)}(i+1)$, a_i is the lower limit value; b_i is the upper limit value; and $\hat{x}^{(0)}(i+1)$ is the forecast of the Grey model.

C. THEORY OF OPTIMIZED GREY-MARKOV MODEL

Based on the drawbacks and shortcomings of the traditional Grey-Markov model, we propose an optimized, equally spaced Grey-Markov model based on problem-oriented thinking [27]. The optimized Grey-Markov model, the RGM-M combination model, is constructed as follows:

After the sixth step of the traditional Grey model processing (reduced by subtraction and reduction), five steps of mathematical calculation are added to improve the prediction accuracy of the model.

(1) Calculate residual sequences $\varepsilon^{(0)}(k)$. The difference between the preliminary fit values of the Grey model and the original data sequence is the residual sequence:

$$\varepsilon^{(0)}(k) = \hat{x}^{(0)}(k) - x^{(0)}(k) \quad (21)$$

(2) Establish and obtain the deviation coefficient λ :

$$\lambda(k) = \frac{[\varepsilon^{(0)}(k)]^2}{\sum_{k=1}^n [\varepsilon^{(0)}(k)]^2} \quad k = 1, 2, \dots, n \quad (22)$$

(3) Calculate the residual correction value $\mu^{(0)}(k)$:

$$\mu^{(0)}(k) = -\lambda \frac{\varepsilon^{(0)}(k)}{|\varepsilon^{(0)}(k)|} \cdot \sum_{k=1}^n |\varepsilon^{(0)}(k)| \quad k = 1, 2, \dots, n \quad (23)$$

(4) The initial fitting data was optimized by the residual correction value to obtain the optimization results $\hat{x}^{(1)}(k)$:

$$\hat{x}^{(1)}(k) = \hat{x}^{(0)}(k) + \mu^{(0)}(k) \quad (24)$$

The residual-corrected Grey model prediction results were used as the initial data of the Markov model [28]. Then, we obtained the optimized Grey-Markov combination model prediction results.

V. RESULTS

A. IPTA TIMING SERIES INSAR RESULTS

To ensure the coherence of the SAR data, IPTA timing series InSAR data were processed in the study area for a one-year period. Our results are shown in Figures 2.

The IPTA timing series InSAR land subsidence results from January 2017 to December 2020 are shown in Figure 3.

After obtaining the timing series InSAR data processing results for the new exploration area in the Weizhou mining area, four typical subsidence points were selected, and each point's land subsidence value sequence was extracted according to a three-month interval. The positions of the

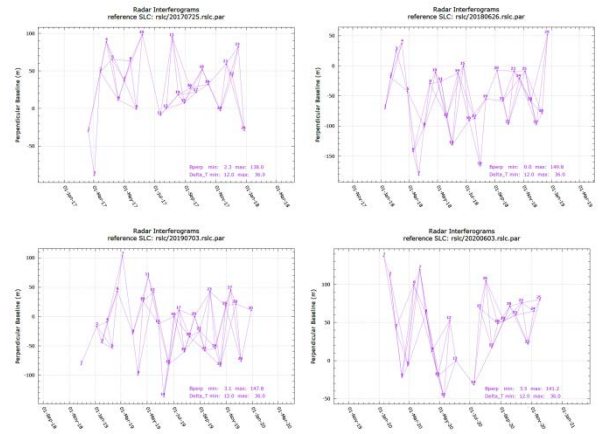


FIGURE 2. Baseline selection diagram of image data.

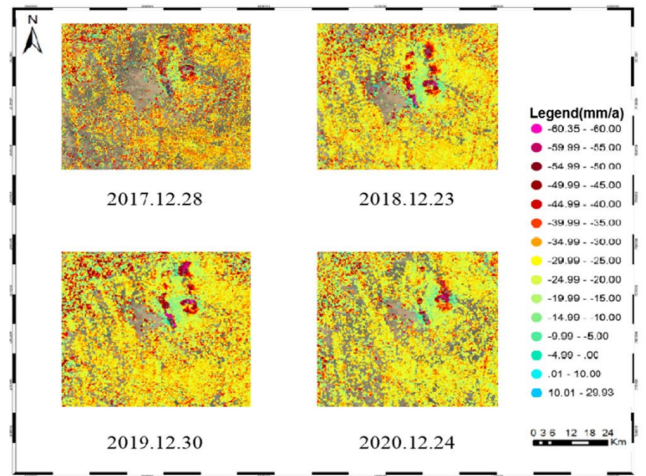


FIGURE 3. IPTA timing series InSAR processing results in the Xinfa exploration area of the Weizhou mining area.

typical subsidence points (P1-P4) and GPS monitoring points (G1-G4) are shown in Figure 4.

The subsidence values of the four typical subsidence points in the new exploration area were compared to the monitoring values of the adjacent GPS monitoring points in the same period, and the temporal subsidence sequence comparison results were obtained, as shown in Figures 5-8.

From these figures, it can be seen that the settlement is large from April 2017 to July 2017, and with the passage of time, the settlement of each phase gradually tends to be stable. This is because there is residual subsidence after mining in the mining area. After mining, there will be subsidence on the surface. At first, the subsidence is large, and then it tends to be stable.

The subsidence values of the four typical subsidence points in the new exploration area were also compared to the monitoring values of the adjacent GPS monitoring points in the same period. The GPS data was used as the ratio to obtain InSAR monitoring accuracy, as shown in Table 3.

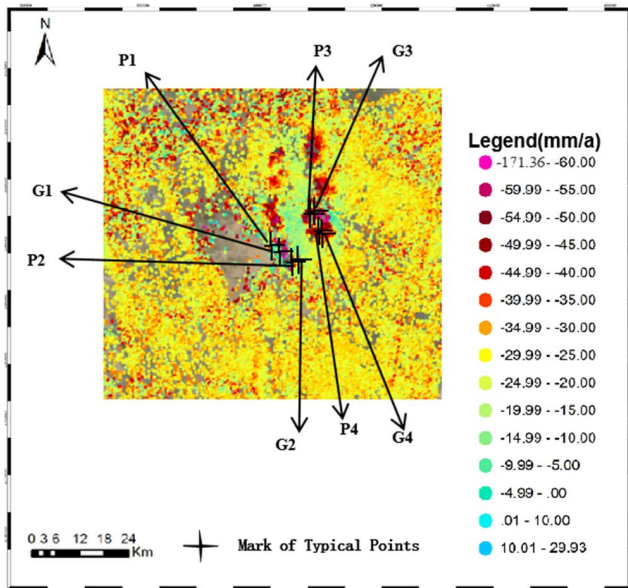


FIGURE 4. Selection locations of typical subsidence points and GPS monitoring points.

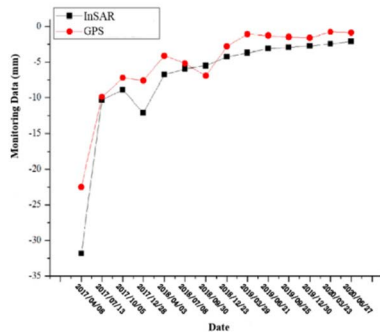


FIGURE 5. Comparison of timing subsidence data of typical point P1 and GPS monitoring point G1.

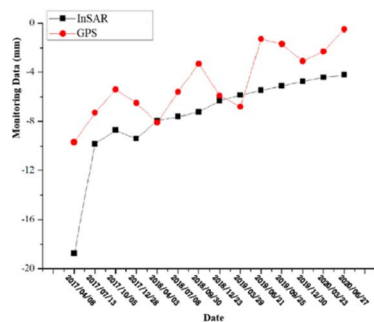


FIGURE 6. Comparison of timing subsidence data of typical point P2 and GPS monitoring point G2.

B. ANALYSIS OF GREY MODEL PREDICTION RESULTS

According to the time series subsidence data for the four typical subsidence points selected in the study area, the original data sequence processed by IPTA timing series InSAR data

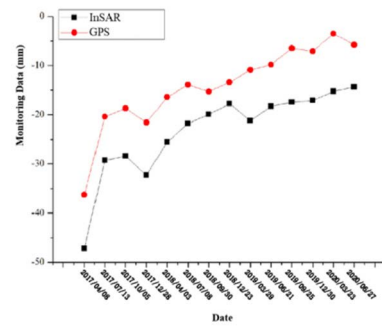


FIGURE 7. Comparison of timing subsidence data of typical point P3 and GPS monitoring point G3.

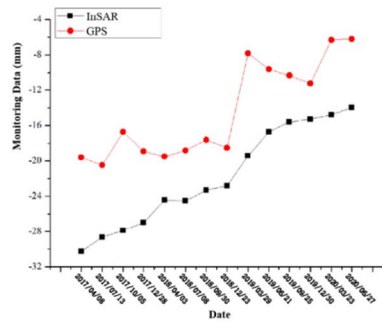


FIGURE 8. Comparison of timing subsidence data of typical point P4 and GPS monitoring point G4.

TABLE 3. InSAR monitoring for data analysis.

Monitoring Points	RMSE (mm)
P1	3.16
P2	3.57
P3	9.28
P4	7.75

was first fitted into the traditional GM (1,1) model. The fitting results are shown in Figures 9-12.

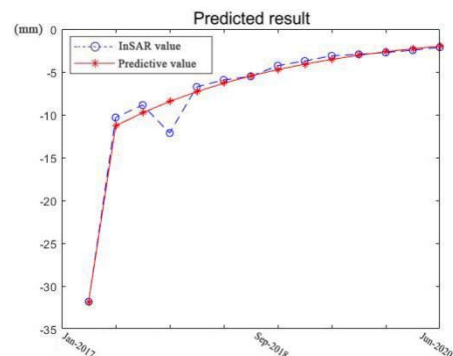


FIGURE 9. Results of Grey model fitting of subsidence data at the P1 point.

The original data sequence on timing had a roughly exponential distribution of subsidence value prediction

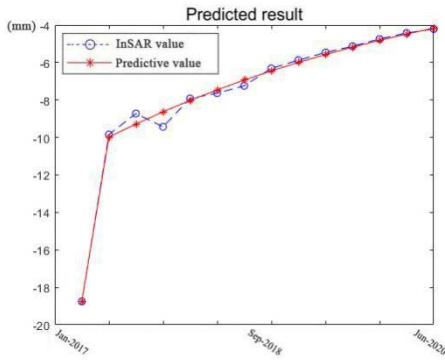


FIGURE 10. Results of Grey model fitting of subsidence data at the P2 point.

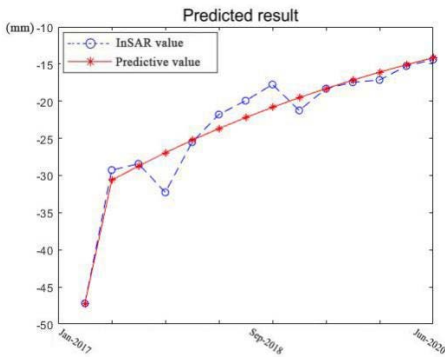


FIGURE 11. Results of Grey model fitting of subsidence data at the P3 point.

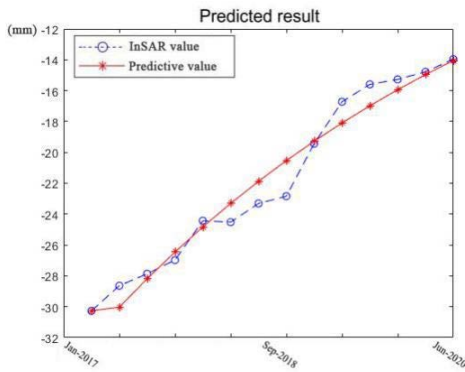


FIGURE 12. Results of Grey model fitting of subsidence data at the P4 point.

(P1 and P2). The traditional Grey model’s fitting prediction accuracy was relatively high, and the fluctuation trend was minor. For the subsidence points (P3 and P4) with high data volatility, the deviation between the predicted value and actual subsidence value was more apparent when the data fluctuated greatly or when the subsidence mutation occurred. Therefore, the single traditional GM (1,1) model only applies to the data series in more apparent exponential distribution trends; and cannot accurately predict the subsidence data sequence with strong volatility.

C. GREY-MARKOV MODEL PREDICTION RESULTS

The data sequence of four typical subsidence points optimized by the GM (1,1) model was used as the initial data sequence of the Markov model, which was replaced with the Markov model. The prediction results of the Grey-Markov combination model were then obtained. The fitted prediction results are shown in Figures 13-16.

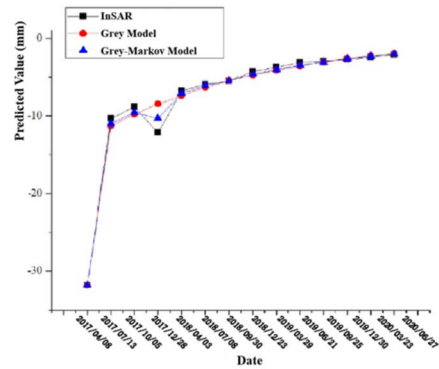


FIGURE 13. Grey-Markov model prediction result of the P1 point subsidence data.

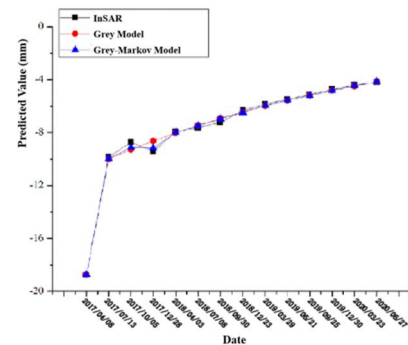


FIGURE 14. Grey-Markov model prediction result of the P2 point subsidence data.

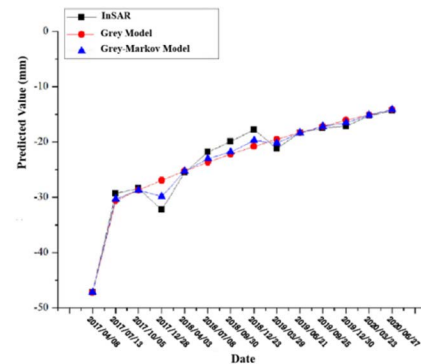


FIGURE 15. Grey-Markov model prediction result of the P3 point subsidence data.

According to the above prediction results, the traditional GM (1,1) model can effectively predict the development

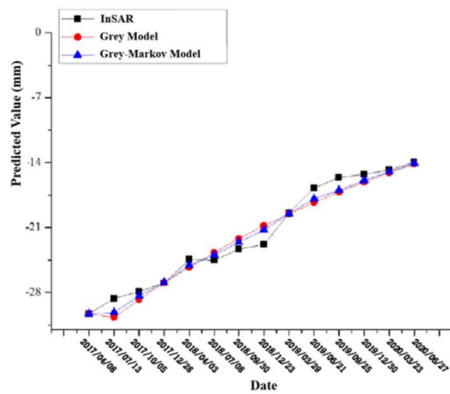


FIGURE 16. Grey-Markov model prediction result of the P4 point subsidence data.

trend of the subsidence data sequence. However, when strong data fluctuations were encountered, the prediction accuracy decreased significantly. The Grey-Markov combination model can analyze the subsidence data while retaining the prediction trend of the Grey model, effectively capturing the fluctuation and subsidence value obtained by IPTA timing series InSAR (raw data used for prediction). Regarding strong fluctuations, the prediction value of the traditional Grey-Markov combination model still has insufficient prediction accuracy.

D. OPTIMIZED GREY-MARKOV MODEL PREDICTION ANALYSIS

The subsidence data sequence obtained through IPTA timing series InSAR data processing was inserted into the optimized residue correction and dynamically assigned Grey-Markov model to fit the RGM-M model. The prediction value comparison results with the traditional Grey-Markov model are shown in Figures 17-20.

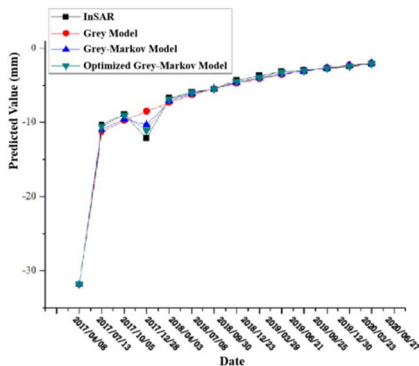


FIGURE 17. Fitting and comparison results of the P1 point subsidence data.

According to the model fitting curve comparison diagram of each typical subsidence point, GM (1,1) model can effectively predict the change trend of data series development, but for some volatile data sequences, its prediction accuracy

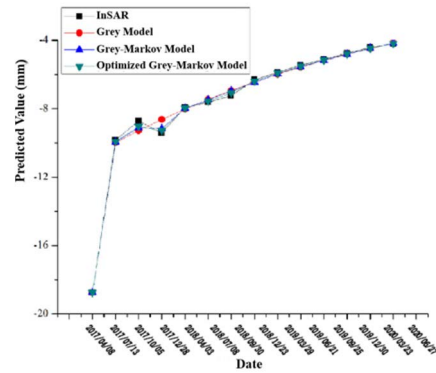


FIGURE 18. Fitting and comparison results of the P2 point subsidence data.

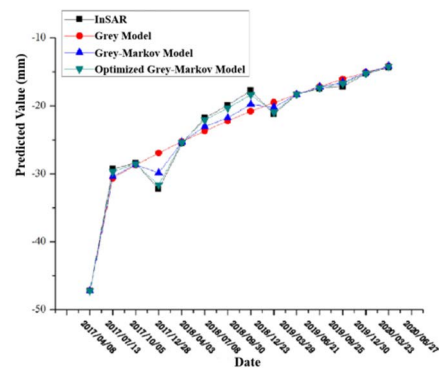


FIGURE 19. Fitting and comparison results of the P3 point subsidence data.

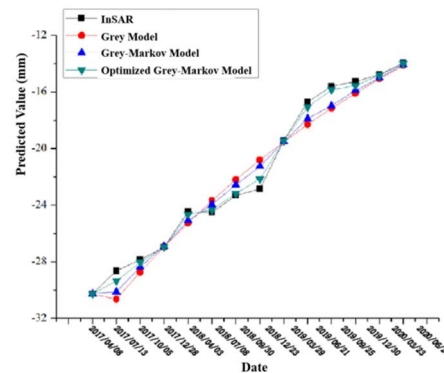


FIGURE 20. Fitting and comparison results of the P4 point subsidence data.

is obviously insufficient. The Grey-Markov combined prediction model predicted the fluctuation changes more accurately based on the Grey model; however, its prediction accuracy must be improved. Compared with the traditional Grey-Markov model, the improved RGM-M model with residual residue correction and dynamic assignment significantly improved the prediction accuracy of the data sequence, which is closest to the measured data sequence in the mining area.

According to the phase 14 data for points P1, P2, P3, and P4 in the new exploration area of the Weizhou mining

area, the subsidence value of the following two periods was predicted, and its accuracy compared to the measured value. The prediction results are shown in Tables 4-7.

TABLE 4. Subsidence data prediction of P1 point.

Time	Initial Data (mm)	RGM-M Model (mm)	Prediction Accuracy	RMSE (mm)
2020.07-2020.09	-1.97	-2.03	97.04%	0.065
2020.09-2020.12	-1.75	-1.82	96.15%	

TABLE 5. Subsidence data prediction of P2 point.

Time	Initial Data (mm)	RGM-M Model (mm)	Prediction Accuracy	RMSE (mm)
2020.07-2020.09	-3.18	-3.31	96.07%	0.125
2020.09-2020.12	-2.97	-3.09	96.11%	

TABLE 6. Subsidence data prediction of P3 point.

Time	Initial Data (mm)	RGM-M Model (mm)	Prediction Accuracy	RMSE (mm)
2020.07-2020.09	-10.37	-9.48	91.42%	0.687
2020.09-2020.12	-8.95	-8.56	95.64%	

TABLE 7. Subsidence data prediction of P4 point.

Time	Initial Data (mm)	RGM-M Model (mm)	Prediction Accuracy	RMSE (mm)
2020.07-2020.09	-11.05	-10.27	92.94%	0.751
2020.09-2020.12	-9.16	-8.44	92.14%	

After developing the prediction of the timing subsidence data for four typical subsidence points in the new exploration and Koizumi exploration areas, we compared the predicted value with the measured value. The prediction accuracy exceeded 90% of the RGM-M model in the study area, and the maximum absolute value of the prediction error was 0.89 mm, showing that the RGM-M model had a higher prediction accuracy and good application prospects in the mining area's land subsidence prediction.

VI. DISCUSSION

According to the shortcomings of the traditional Grey-Markov model, we theoretically improved the mathematical optimization; and prediction accuracy of the Grey model and the Grey-Markov combination model. The optimized

RGM-M model constructed here has the following advantages compared with the traditional Grey-Markov model:

(1) The RGM-M model proposes a new residual correction method for the Grey model, which optimizes and improves the residual weight. The data prediction accuracy is greatly improved compared with the traditional Grey model. Previous residual-corrected grey models; were mostly optimized for residual sequence or used other model optimized residual correction methods. However, in practice, its raw data sequence may not satisfy the ideal exponential distribution since some emergent, and uncontrollable factors can affect land subsidence data. There is inevitable volatility in the raw data of the time series. Therefore, its residual sequence is not necessarily the ideal application situation for the Grey model. Therefore, the grey model fit was optimized again. In theory, there is a certain limit to its applicability. The residual correction model was optimized according to the residual weight and can theoretically be improved by the original data sequence according to different original data sequence conditions, improving the prediction accuracy of the Grey model.

(2) A weighted Markov model with dynamic empowerment was developed for the mine land subsidence data volatility. Compared to the traditional Markov model, its evaluation weight matrix is determined from the initial sequence; and remains fixed in the subsequent predictions; therefore, its prediction inevitably deviates. Dynamic empowerment; and data values after each Grey-Markov model prediction were added to the calculated sample of the next evaluation weight matrix; and a dynamic Markov evaluation weight matrix was established; that was more scientific in theory. In previous weighted Markov models, the prediction data was used in the initial state; and predicted the row vector of the next probability transition matrix based on the last transition probability matrix. The first prediction data produces an accumulation of errors that negatively impact the subsequent prediction. We propose a new dynamic empowerment method; to replace the Markov optimization of the first data value in the data sequence with the Markov initial data sequence and recalculate the new Markov sequence, establishing a dynamic Markov prediction model. Using this method, we would consistently update the evaluation weight matrix and transfer the probability matrix, improving the scientific nature of the model prediction.

(3) The four typical subsidence points in the subsidence data of the new exploration and spring exploration areas were replaced with the traditional GM (1,1) model, Grey-Markov combination prediction model with optimized residual correction, and dynamic empowerment of Grey-Markov combination model. We compared and analyzed the prediction results. Our results show that the Grey-Markov model can more accurately predict the trend and subsidence value of land subsidence than the traditional Grey-Markov combination model, with higher accuracy and a wider application range.

However, there are still some shortcomings:

(1) The research area selected in this paper is a mining area, but the subsidence value is small compared with the general mining area. In particular, the average land subsidence rate and value are lower, which may not fully verify the improved dynamic assignment and residual modified Grey-Markov RGM-M model in broadening the applicable scope of the model and prediction accuracy of the data series.

(2) The data sample of the original data sequence is limited; to some extent, limiting the prediction accuracy of the dynamically empowered Grey-Markov model. If the original monitoring data of the longer time series is used for long-term land subsidence monitoring, a more accurate land subsidence prediction value can be obtained.

VII. CONCLUSION

IPTA timing series InSAR processing technology is used in the new exploration area of the Weizhou mining area. We selected four subsidence points in the mining area, and extracted the temporal land vertical deformation results. We inserted the IPTA timing series InSAR land vertical deformation data of each typical subsidence point into the improved RGM-M Grey-Markov model, completed the subsidence prediction of the typical mining area, compared the prediction data with the traditional Grey model and Grey-Markov combination model, and drew the following conclusions:

(1) By processing and predicting the InSAR data and comparing the vertical deformation data to the adjacent GPS data, the reliability of IPTA timing series InSAR data processing results was verified, demonstrating InSAR technology's strong application in the land deformation monitoring of mining areas.

(2) Aiming at the shortcomings of the traditional grey model and Markov model, we proposed a modified RGM-M Grey-Markov model, which improves its prediction accuracy and expands its applicability. The improved RGM-M model was used to simulate and predict the subsidence data of typical subsidence points from 2017 to 2020. The prediction results were better than the traditional single grey model and Grey-Markov combination model. Therefore, the improved RGM-M model has important guiding significance and application prospects for land subsidence monitoring, prediction, and safety management in mining areas.

REFERENCES

- [1] D. Yuan, C. Geng, L. Zhang, and Z. Zhang, "Application of gray-Markov model to land subsidence monitoring of a mining area," *IEEE Access*, vol. 9, pp. 118716–118725, 2021, doi: [10.1109/ACCESS.2021.3106144](https://doi.org/10.1109/ACCESS.2021.3106144).
- [2] F. Cigna and D. Tapete, "Sentinel-1 big data processing with P-SBAS InSAR in the geohazards exploitation platform: An experiment on coastal land subsidence and landslides in Italy," *Remote Sens.*, vol. 13, no. 5, p. 885, Feb. 2021.
- [3] A. Ferretti, C. Prati, and F. Rocca, "Permanent scatterers in SAR interferometry," *IEEE Trans. Geosci. Remote Sens.*, vol. 39, no. 1, pp. 8–20, Jan. 2001.
- [4] D. Zhou, A. Simic-Milas, J. Yu, L. Zhu, B. Chen, and N. Muhetaer, "Integrating RELAX with PS-InSAR technique to improve identification of persistent scatterers for land subsidence monitoring," *Remote Sens.*, vol. 12, no. 17, p. 2730, Aug. 2020.
- [5] W. Ge, Y. Li, Z. Wang, C. Zhang, and H. Yang, "Spatial-temporal ground deformation study of Baotou based on the PS-InSAR method," *Acta Geologica Sinica English Ed.*, vol. 95, no. 2, pp. 674–683, Apr. 2021.
- [6] O. Beladam, T. Balz, B. Mohamadi, and M. Abdalhak, "Using PS-InSAR with Sentinel-1 images for deformation monitoring in Northeast Algeria," *Geosciences*, vol. 9, no. 7, p. 315, Jul. 2019.
- [7] Y. Liu, C. Zhao, Q. Zhang, and C. Yang, "Complex surface deformation monitoring and mechanism inversion over Qingxu-Jiaocheng, China with multi-sensor SAR images," *J. Geodynamics*, vol. 114, pp. 41–52, Feb. 2018.
- [8] A. Abdel-Hamid, O. Dubovyk, and K. Greve, "The potential of sentinel-1 InSAR coherence for grasslands monitoring in Eastern Cape, South Africa," *Int. J. Appl. Earth Observ. Geoinf.*, vol. 98, Jun. 2021, Art. no. 102306.
- [9] G. Giardina, P. Milillo, M. J. DeJong, D. Perissin, and G. Milillo, "Evaluation of InSAR monitoring data for post-tunnelling settlement damage assessment," *Struct. Control Health Monitor.*, vol. 26, no. 2, p. e2285, Feb. 2019.
- [10] L. Zhang et al., "Detection of minor differential transformation of active break in Tangshan City based on multi-source SAR data," *Remote Sens. Land Resour.*, vol. 32, no. 3, pp. 114–120, 2020.
- [11] A. Galdelli, A. Mancini, C. Ferrà, and A. N. Tassetti, "A synergic integration of AIS data and SAR imagery to monitor fisheries and detect suspicious activities," *Sensors*, vol. 21, no. 8, p. 2756, Apr. 2021.
- [12] Y. You, R. Wang, and W. Zhou, "A phase filter for multi-pass InSAR stack data by hybrid tensor rank representation," *IEEE Access*, vol. 7, pp. 135176–135191, 2019, doi: [10.1109/ACCESS.2019.2942008](https://doi.org/10.1109/ACCESS.2019.2942008).
- [13] W. Zhou et al., "A combined model prediction method for surface subsidence monitoring in mining areas," *Geodey Geodyn.*, vol. 41, no. 3, pp. 308–312, 2021.
- [14] O. Orhan, "Monitoring of land subsidence due to excessive groundwater extraction using small baseline subset technique in Konya, Turkey," *Environ. Monitor. Assessment*, vol. 193, no. 4, pp. 1–17, Apr. 2021.
- [15] H. Jiang, T. Balz, F. Cigna, and D. Tapete, "Land subsidence in Wuhan revealed using a non-linear PSInSAR approach with long time series of COSMO-SkyMed SAR data," *Remote Sens.*, vol. 13, no. 7, p. 1256, Mar. 2021.
- [16] Z. Zhenchao et al., "Application of the time-varying parameter GM (1,1) in railway settlement," *Surv. Mapping Sci.*, vol. 45, no. 3, pp. 39–45, 2020, doi: [10.16251/j.cnki.1009-2307.2020.03.007](https://doi.org/10.16251/j.cnki.1009-2307.2020.03.007).
- [17] H.-P. Zhang and Q.-H. Chen, "Research on the prediction of network public opinion based on Grey-Markov model," *Inf. Sci.*, vol. 36, no. 1, pp. 75–79, 2018.
- [18] R. Wang, W. Song, L. Liu, C. Du, and X. Zhao, "Prediction of fire smoke concentration based on Grey-Markov model," in *Proc. IEEE 9th Int. Conf. Electron. Inf. Emergency Commun. (ICEIEC)*, Jul. 2019, pp. 1–5.
- [19] W. Zhang, "Analysis of sports training injury measurement with Grey-Markov model (GMM)," in *Proc. 10th Int. Conf. Measuring Technol. Mechatronics Autom. (ICMTMA)*, Feb. 2018, pp. 194–197, doi: [10.1109/ICMTMA.2018.00054](https://doi.org/10.1109/ICMTMA.2018.00054).
- [20] K. J. Reinders, R. F. Hanssen, F. J. van Leijen, and M. Korff, "Augmented satellite InSAR for assessing short-term and long-term surface deformation due to shield tunnelling," *Tunnelling Underground Space Technol.*, vol. 110, Apr. 2021, Art. no. 103745.
- [21] G. Zhao, H. Zhang, and X. Qin, "Prediction of grain humidity based on improved Grey-Markov model," in *Proc. IEEE Symp. Ser. Comput. Intell. (SSCI)*, Dec. 2019, pp. 2933–2939, doi: [10.1109/SSCI44817.2019.9003000](https://doi.org/10.1109/SSCI44817.2019.9003000).
- [22] E. Schindler and M. O. Karlsson, "A minimal continuous-time Markov pharmacometric model," *AAPS J.*, vol. 19, no. 5, pp. 1424–1435, Sep. 2017.
- [23] Z. Zhou, B. Lan, Z. Huang, P. Chen, X. Deng, W. Mao, and L. Yuan, "The application of Grey-Markov forecasting model based on entropy method," in *Proc. 37th Chin. Control Conf. (CCC)*, Jul. 2018, pp. 1533–1538.
- [24] S. Wang, Q. Zhai, and L.-N. Xu, "Prediction on Chinese female middle-long-distance results based on Grey-Markov model," *Tech. Rep.*, 2016, pp. 61–162.

- [25] R. Wang, W. Song, L. Liu, C. Du, and X. Zhao, "Prediction of fire smoke concentration based on Grey-Markov model," in *Proc. IEEE 9th Int. Conf. Electron. Inf. Emergency Commun. (ICEIEC)*, Jul. 2019, pp. 1–5.
- [26] J. P. S. Gonçalves, F. Fruett, J. G. Dalfré Filho, and M. Giesbrecht, "Faults detection and classification in a centrifugal pump from vibration data using Markov parameters," *Mech. Syst. Signal Process.*, vol. 158, Sep. 2021, Art. no. 107694.
- [27] F. Yuan and Y. Mingda, "A Grey-Markov chain prediction model with value correction for state intervals," *Surv. Geographic Inf.*, vol. 46, no. 4, pp. 65–68, 2021, doi: [10.14188/j.2095-6045.2019107](https://doi.org/10.14188/j.2095-6045.2019107).
- [28] L. Feilong, "Study of the Markov-transformed integer-valued time-series models," Jilin Univ., Changchun, China, Tech. Rep., 2021, doi: [10.27162/d.cnki.gjlin.2021.003314](https://doi.org/10.27162/d.cnki.gjlin.2021.003314).



DEBAO YUAN was born in April 1976. He received the Ph.D. degree in geodesy and surveying engineering from the China University of Mining and Technology (Beijing), in 2009. He has been an Associate Professor with the China University of Mining and Technology (Beijing), a Master's Supervisor, and the Director of Surveying and Mapping. He is the author of two books, more than 40 articles, and two inventions. He has participated in the completion of two National Natural Science Fund projects and one of 1973 sub-projects. His research interests include GPS positioning and navigation, deformation disaster monitoring and data processing, 3S integration and application, 3-D laser measurement technology and its application, UAV disaster monitoring, and data processing. His awards include the second prize of Beijing Higher Education and Teaching Achievement Award, the second prize of Geographic Information Technology Progress Award, and the second prize of Coal Industry Education and Teaching Achievement Award.



LIBIAO ZHANG was born in Pingyao, Shanxi, China, in December 1997. He received the bachelor's degree from the China University of Mining and Technology, in 2020. He is currently pursuing the degree with the School of Earth Science and Surveying and Mapping Engineering, China University of Mining and Technology (Beijing).

His research interests include deformation monitoring data processing and InSAR landslide deformation monitoring.

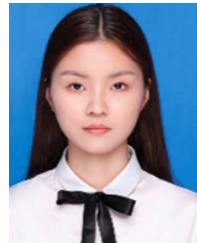


RUOPENG YAN was born in Jinzhong, Shanxi, China, in 1996. He received the bachelor's degree majoring in geographic informatics from Taiyuan Normal University. He is currently pursuing the degree with the School of Earth Science and Surveying and Mapping Engineering, China University of Mining and Technology (Beijing).

His research direction during the postgraduate period is InSAR data processing.



LING WU was born in December 1998. She is currently pursuing the degree in surveying and mapping science and technology with the China University of Mining and Technology (Beijing).



YANYAN FENG was born in Zhumadian, Henan. She is currently pursuing the degree majoring in surveying and mapping engineering with the School of Earth Science and Surveying and Mapping Engineering, China University of Mining and Technology (Beijing).



LUYI FENG is currently pursuing the degree with the School of Earth Science and Surveying and Mapping Engineering, China University of Mining and Technology (Beijing). He is a 20th-level Remote Sensing Student.

...